



Biocompatibility and neurotoxicity of magnesium alloys potentially used for neural repairs



Jianjun Fei^{a,b,1}, Xiaoxiao Wen^{a,1}, Xiao Lin^{a,*,1}, Saijilafu^{a,c}, Weihua Wang^a, Olga Ren^d, Xinjian Chen^b, Lili Tan^e, Ke Yang^{e,**}, Huilin Yang^{a,c}, Lei Yang^{a,c,***}

^a Orthopaedic Institute, Department of Orthopaedics, The First Affiliated Hospital, Soochow University, Suzhou, Jiangsu Province 215006, China

^b School of Electronics and Information Engineering, Soochow University, Suzhou, Jiangsu Province 215006, China

^c International Research Center for Translational Orthopaedics (IRCTO), Soochow University, Suzhou, Jiangsu Province 215006, China

^d Departments of Biology, Honours Biomedical Science, University of Waterloo, Canada

^e Institute of Metal Research, Chinese Academy of Sciences, Shenyang, Liaoning Province 110016, China

ARTICLE INFO

Article history:

Received 17 December 2016

Accepted 18 April 2017

Available online 20 April 2017

Keywords:

Nerve repair

Magnesium alloys

Biodegradation

Dorsal root ganglion

Biocompatibility

ABSTRACT

Nerve injury, especially the large-size nerve damage, is a serious problem affecting millions of people. Entubulation of two ends of the injured nerve by using an implantable device, *e.g.*, nerve guidance conduit (NGC), to guide the regeneration of nerve tissue is a promising approach for treating the large-size nerve defect. Magnesium (Mg) and its alloys are biodegradable, conductive, and own good mechanical properties. Mg²⁺ ion, one of the main degradation products of Mg and its alloys, was reported to promote the proliferation of neural stem cells and their neurite production. Thus, Mg and its alloys are potential materials for fabricating the nerve repair implants, such as NGC or scaffold. However, the compatibility of Mg alloys to cells, especially neurons is not clear. In this work, NZ20 (Mg-2Nd-Zn), ZN20 (Mg-2Zn-Nd) and Mg-10Li magnesium alloys were selected for study, due to the improved mechanical properties of NZ20 and ZN20 alloys and bio-function of Li⁺ ions from Mg-10Li to nervous system, respectively. The degradation behavior and biocompatibility were studied by *in vitro* degradation test and cell adhesion assay, respectively. Specifically, the cytocompatibility to dorsal root ganglion (DRG) neurons, RF/6A choroid-retina endothelial cells, and osteoblasts in the cell culture media containing Mg alloy extracts were investigated. The results showed that Mg alloys degraded at different rates in cell culture media and artificial cerebrospinal fluid. The three alloy extracts showed negligible toxic effects on the endothelial cells and osteoblasts at short term (1 day), while NZ20 extract inhibited the proliferation of these two types of cells. The effect of Mg alloy extracts on cell proliferation was also concentration-dependent. For DRG neurons, ZN20 and Mg-10Li alloy extracts showed no neural toxicity compared with control group. The results of the present work show a potential and feasibility of Mg-10Li and ZN20 for nerve repair applications.

© 2017 Elsevier B.V. All rights reserved.

1. Introduction

Nerve injury, including both periphery nervous system (PNS) and central nervous system (CNS) injuries, is a serious and debilitating condition that affects a large number of people worldwide. Besides pathological consequences of nerve injury on patients, it also causes considerably high healthcare expenditure, reduced employer output and loss of

earnings. There are a number of clinical treatments for nerve injuries. For small nerve injury gaps, the coaptation of the two severed nerve ends *via* direct suturing is a common method. For larger gaps, a common approach is to use an implantable entubulation device, *e.g.*, nerve guidance conduit (NGC), to guide the regeneration of nerve tissue. Optimal NGC should simultaneously supply a contact guidance, proper microenvironment and protection for the repair of nerve tissue. With proper configuration and composition, the NGC would enhance the axonal regeneration [1,2]. Some NGCs, such as single hollow tubes, are commercially available for the connection of transected peripheral nerves. However, their clinical outcomes are still questionable. Current materials used in the nerve repairs are mainly organics, including extracellular matrix (ECM), natural polysaccharide and protein, and synthetic polymers [3–5]. Their ability or efficacy for large-gap repair (such as beyond 20 mm) is very limited and there is an urgent need for exploration of new nerve repair materials.

* Correspondence to: X. Lin, Room 318 Building #1, South Campus of Soochow University, 708 Renmin Road, Suzhou, Jiangsu Province 215006, China.

** Correspondence to: K. Yang, Institute of Metal Research, 72 Wenhua Road, Shenyang, Liaoning Province 110016, China.

*** Correspondence to: L. Yang, Room 313 Building #1, South Campus of Soochow University, 708 Renmin Road, Suzhou, Jiangsu Province 215006, China.

E-mail addresses: xlina@suda.edu.cn (X. Lin), kyang@imr.ac.cn (K. Yang),

leiy@suda.edu.cn (L. Yang).

¹ These authors contribute equally to this work.

Mg alloys were recently extensively studied as new biodegradable metallic materials [6–9] with degradation product mainly consisting of Mg^{2+} ions. The Mg alloys are reported to have several specific advantages over polymeric materials for the NGC application. Firstly, Mg alloys can release bio-functional metallic ions that promote the nerve repair. Previous studies have shown the positive effects of Mg^{2+} ions on the nerve cells and nervous system both *in vitro* and *in vivo* [10,11]. The Mg^{2+} ions were found to play an important role in the repairs of both peripheral nerve and spinal cord injury. For instance, Mg supplement promoted rat sciatic nerve regeneration and down-regulated inflammatory response after nerve crush injury [4]. In addition, $MgSO_4$ showed vaso- and neuro protective properties after a contusion injury to the rat spinal cord [12] and proper concentration of Mg^{2+} ions could promote the proliferation of neural stem cells [13]. Addition of Mg salt solution could also enhance cell density and neurite production of primary mouse neuronal stem cells [14]. Thus, the degradation of Mg alloy implant is expected to supply a favorable ionic environment for nerve repair or regeneration. Furthermore, other metallic elements that are beneficial to nerve regeneration (such as Li) could be alloyed with Mg to facilitate the nerve repair. Secondly, Mg alloys are excellent conductor to enhance electrical stimulation or signal transduction in nerve cells, which reportedly promotes the regeneration of injured nerves. For example, electrical stimulation could greatly promote the neurite outgrowth of cultured dorsal root ganglion neurons [15]. Recently, conductive hydrogels have been electrically coupled with nerve cells to achieve efficient electrical stimulation and potential promotion of neuronal outgrowth [16]. Thirdly, Mg alloys are significantly more robust than biodegradable organic materials [17–19], which could provide an improved structural support for nerve regeneration or repair [4,5]. Lastly, the degradation rate of Mg alloys can be easily adjusted [18–22] and thus optimized to meet the requirement of nerve repair.

The applications of Mg alloy have been mainly focused on orthopedic devices [23–26] and cardiovascular stents [27], of which the clinical studies have demonstrated the promises [24,27,28]. However, few studies have been focused on utilizing Mg alloy for nerve repair. Recently, Vennemeyer et al. performed a preliminary *in vivo* study to reveal the potential of pure Mg for nerve repair, showing apparent nerve regeneration but no necrosis [29]. However, the biological properties especially neural biocompatibility of Mg alloys has not been well investigated to date. In the present study, cytotoxicity and neural toxicity studies were performed to evaluate the feasibility of Mg alloys for nerve repair. Extruded Mg-2Nd-Zn (NZ20), Mg-2Zn-Nd (ZN20) and rolled Mg-10Li alloys were selected for the present study, corresponding to the varied mechanical properties and the ability to release secondary Li^+ ions, respectively. The degradation properties of the Mg alloys were studied by immersion test in different simulated body fluids, then the cytocompatibility of the Mg alloys was evaluated by osteoblasts and choroid-retina endothelial cells, and finally the neural toxicity was assessed by dorsal root ganglion (DRG) neurons.

2. Materials and methods

2.1. Materials

ZN20 (2 wt% Zn, 0.5 wt% Nd, Mg in balance), NZ20 (2wt.%Nd, 0.2 wt% Zn, Mg in balance) and Mg-10Li (10 wt% Li, Mg in balance) alloys were selected for study. The extruded ZN20 and NZ20 alloys with extrusion ratio of 64:1 were supplied by Institute of Metal Research, CAS. The rolled Mg-10Li alloy was purchased from Zhengzhou Research Institute of CHALCO. For all the experiments, ZN20 and NZ20 alloy tablets with diameter of 10 mm and thickness of 4 mm, and Mg-10Li squares with size of $10 \times 10 \times 1 \text{ mm}^3$ were used. Before experiments, the alloy samples were successively polished on various grade SiC papers up to 2000 grit finish and then ultrasonically cleaned.

For microstructure characterization, Mg alloys were successively polished on various grade SiC papers up to 2000 grit finish. Then the

samples were polished with 2.5 μm and 0.5 μm polishing paste, respectively. Microstructure of the Mg alloys was examined by scanning electron microscopy (SEM, Quanta 250, FEI) after acid etching.

2.2. *In vitro* biodegradation tests

In vitro biodegradation tests were performed by immersion approach using three physiological fluids at an immersion ratio of 1.25 cm^2/ml (material surface area to liquid volume). Dulbecco's Modified Eagle Medium (DEME, Hyclone™, GE healthcare life sciences), DMEM with 10 vol% fetal bovine serum (FBS Gibico®, Life technologies™), and house-prepared artificial cerebrospinal fluid (aCSF) were used. The aCSF was prepared by dissolving 124 mM NaCl, 5 mM KCl, 1.25 mM NaH_2PO_4 , 2 mM MgSO_4 , and 10 mM glucose in deionized water and then inflating the gas of 5 vol% $\text{CO}_2/95 \text{ vol}\% \text{ air}$. 2 mM CaCl_2 was then added in the solution after 5 min and 26 mM NaHCO_3 was added after 10 min.

Alloy samples were immersed in the physiological fluids and incubated at 37 °C. The pH of fluids was recorded every two days to reflect the degradation progress [30]. The fluids were also replaced by fresh ones after the pH measurement, mimicking the situation of *in vivo* circulation of body fluids. The net weight of each sample was measured at the end of the immersion test and three replicates were tested for each Mg alloy.

2.3. Cytocompatibility tests

2.3.1. Cells and material extracts

MC3T3-E1 osteoblasts and RF/6A choroid-retina endothelial cells purchased from the Type Culture Collection of Chinese Academy of Sciences (Shanghai, China) were selected for the cyto-compatibility tests. DMEM with 10 vol% FBS and 1 vol% penicillin-streptomycin solution were used as the cell culture medium. Indirect contact method of culturing the cells with the alloy extracts was used to evaluate the compatibility of alloys to cells. Alloy samples were immersed in 75% ethanol for 15 min for sterilization and then rinsed by phosphate buffer saline (PBS) for three times. After that, the alloy extracts for cell test were prepared by immersing the samples in PBS at an extraction ratio of 1.25 cm^2/ml and incubating in a humidified atmosphere of 5% CO_2 at 37 °C for 1 day. The supernatant was withdrawn and filtrated through 0.22 μm membrane filter (Millex-GP, Millipore) before cell tests.

2.3.2. LIVE/DEAD viability assay

Osteoblasts and choroid-retina endothelial cells were first cultured in the regular cell culture medium (DMEM with 10 vol% FBS and 1 vol% penicillin-streptomycin solution) at a density of 5000 cells/ cm^2 in a 24-well plate. After 4 h, the cell culture media in each well were replaced by 1 mL mixed media with 25 vol% alloy extracts and 75 vol% regular cell culture media. Regular cell culture medium with 25 vol% PBS was used as a control and each sample had 4 replicas. Cells were cultured in a humidified atmosphere of 5% CO_2 at 37 °C. After one day of culture, the cells were stained by LIVE/DEAD® assay (Invitrogen) according to manufacturer's instructions. Briefly, the mixed solution of Calcein-AM and Ethidium homodimer was added to each well and incubated for 30 min. After then, the solution was removed and the cells were observed under a fluorescence microscope (EVOS, AMG). The living and dead cells were stained by Calcein-AM and Ethidium homodimer into green and red colors, respectively.

For the purpose of quantitative analysis, 8 images from 4 replicas in each group were randomly selected. The numbers of live and dead cells in each well were counted for further calculation and statistics.

2.3.3. CCK-8 proliferation assay

Osteoblasts and choroid-retina endothelial cells were seeded onto the 96-well plate at a seeding density of 5000 cells per well and cultured for 1 day. After then, the cell culture media were replaced by 200 μL

regular cell culture medium containing 25 vol% alloy extracts. Regular cell culture medium containing 25 vol% PBS was used as control.

The ZN20 alloy extracts were used as an example to study the concentration dependence of toxicity of alloy extracts. The cell culture media of some wells were replaced with mixture of ZN20 extracts and regular cell culture media with alloy extracts concentration ranging from 12.5 vol% to 66.7 vol%. The regular cell culture media with 12.5 vol% PBS was used as a control.

After prescribed times, cell culture medium in each well was removed and the well was rinsed by 200 μL PBS for two times. 10 μL CCK-8 (Dojindo Molecular Technologies, Inc) mixed in 100 μL PBS was then added to each well and incubated at 37 °C for 2 h. After incubation, the solution was transferred out to a new 96-well plate. The optical density (O.D.) of the solution in each well was measured on a micro-plate reader (Power Wave X, BioTek) at a wavelength of 450 nm. The O.D. value was positively correlated with the cell number in the well, reflecting the state of cell proliferation. Five replicas were tested for each alloy extracts.

2.4. *In vitro* neural toxicity test

2.4.1. Culturing DRG neurons with alloy extracts

The neural toxicity of Mg alloys was studied by the assessment of neurite outgrowth of DRG cells in the presence of alloy extracts which were prepared by immersing the Mg alloys in the Minimum Essential Media (MEM, Invitrogen) in a humidified atmosphere of 5% CO_2 at 37 °C for 24 h. The study was approved by the animal ethics committee and ICUC committee at Soochow University following the international regulatory treaty (Documentation numbers NSFC81622032). DRG neurons from 6-week old Sprague Dawley rats were excised and seeded on 12-mm round coverslips placed in 24-well plates at a density of 1000 cells per well. The coverslips were precoated with 100 $\mu\text{g}/\text{mL}$ Poly-D-Lysine (Sigma-Aldrich) and 10 $\mu\text{g}/\text{mL}$ Laminin (Invitrogen) for 2 h. DRG neurons were first cultured in MEM medium (Invitrogen) supplemented with 5% fetal bovine serum, 100 U/ml penicillin, 100 $\mu\text{g}/\text{mL}$ streptomycin and the antimetabolic reagents containing 20 μM 5-fluoro-2-deoxyuridine (Sigma-Aldrich) and 20 μM uridine (Sigma-Aldrich). When neurons had attached to the substrates after 4 h incubation, the cell culture medium was replaced by the alloy extracts and cultured for another 3 days. DRG neurons cultured in the regular cell culture media were set as controls.

2.4.2. Immunostaining of DRG neurons

DRG neurons were cultured for 3 days and processed for immunocytochemistry by fixing with 4% paraformaldehyde (Sigma) at room temperature for 20 min and rinsing with PBS. 200 μL blocking solution (0.1% Triton X-100 and 2.0% bovine serum albumin in PBS) was added to the fixed neurons for 60 min at room temperature. Neurons were further incubated with primary antibody solution (1:1200 dilution in PBS for the mouse anti- β III-tubulin antibody) for 60 min at room temperature. After that, DRG neurons were rinsed with PBS and incubated with the corresponding secondary antibodies (goat anti-mouse IgG) for 60 min at room temperature in the dark. After a final rinse with PBS, DRG neurons were observed by fluorescence microscopy (Axio Imager M1, Zeiss).

For the purposes of a quantitative analysis, 10 DRG neurons in each group were randomly selected, and the length of neurite was measured using NIH ImageJ software (National Institute of Health, Bethesda, MD, USA). The longest neurite of each neuron was recorded for further analysis.

2.4.3. Measurements of pH and ion concentration

The pH values and concentrations of Mg^{2+} , Ca^{2+} and Li^+ ions in the alloy extracts for culturing DRG neurons were measured by a pH meter (Lei-ci, INESA Scientific Instrument Co., Ltd) and atomic absorption spectrometer (AAS, AA800, Perkin Elmer), respectively. For the AAS

test, standard solutions with 100 ppm of Mg^{2+} , Ca^{2+} and Li^+ ions were used as references and the concentrations of Mg^{2+} , Ca^{2+} and Li^+ ions were calculated based on the relative absorption intensities to those of references. The average value of three parallel samples of each alloy extracts was calculated.

2.5. Statistics

Data of the biological tests were reported as the mean \pm SD (standard deviation) calculated from repeated test. Statistical analysis was conducted by one-way analysis of variance (one way-ANOVA). All the pair wise comparisons were performed by the *post hoc* test of Turkey. When *P* value was <0.05, significant differences were determined.

3. Results

3.1. Microstructure analysis of the Mg alloys

The typical microstructure of ZN20, NZ20 and Mg-10Li alloys was shown in Fig. 1. The grain sizes of extruded ZN20 and NZ20 alloys were similar but significantly smaller than that of Mg-10Li alloy. In addition, NZ20 alloy had more grain boundary phase than ZN20 alloy and there were oxides particles on the surface of Mg-10Li alloy.

3.2. Degradation of Mg alloys in simulated physiological fluids

Fig. 2(a)–(c) shows the pH value changes of different simulated physiological fluids containing ZN20, NZ20 and Mg-10Li alloys for 14 days, respectively. The pH of all the fluids significantly changed to basic regime due to the well-known release of hydroxyl as a result of Mg alloy degradation. It is well known that the changes in pH value of immersion fluids indicate the degradation rates of the alloys [30]. Clearly, pH values of all the three fluids followed the sequence: Mg-10Li > NZ20 > ZN20 at most of the time points, indicating that Mg-10Li and ZN20 had the highest and lowest degradation rates in all the three fluids, respectively. For all the three alloys, the decrease in the pH of DMEM with and without FBS at the later immersion period was probably due to the formation of protective layer composed of deposition and degradation products which retarded the degradation progress [31]. In contrast, no obvious decrease in the pH values of aCSF was observed, possibly due to the lack of reactive ions in aCSF, rendering the formation of protective layer impossible [32]. The results indicate that the Mg alloys have vastly varied degradation behavior in different physiological fluids. Fig. 2(d) shows the weight changes of three Mg alloys immersed in DMEM with FBS, DMEM without FBS, and aCSF, respectively. The increase in weight was attributed to the degradation products and substances in the physiological fluids deposited on the surface. The weight of Mg-10Li alloy changed the most, indicating an active degradation reaction, while the weight of ZN20 alloy showed almost no change in all three physiological fluids due to the slight degradation reaction. However, large deviations in weight changes were observed for all the three alloys, indicating the degradation and deposition of degradation products on the alloy surfaces could be a complicated dynamic balance that varies dramatically in different conditions, e.g., *in vitro* vs. *in vivo*.

3.3. Cyto-compatibility tested by osteoblasts and choroid-retina endothelial cells

Fig. 3(a) shows fluorescence microscopy images of osteoblasts and choroid-retina endothelial cells cultured in 25 vol% alloy extracts for 1 day. The osteoblasts and endothelial cells were viable in the alloy extracts, revealing similar adhesion density and spreading compared to the 25 vol% PBS control group. There were seldom dead cells in the alloy extract groups, also similar to that of PBS control. Quantitative results of live and dead cells density of different alloy extracts are shown in Fig. 3(b). The density of live osteoblasts in NZ20 groups was slightly

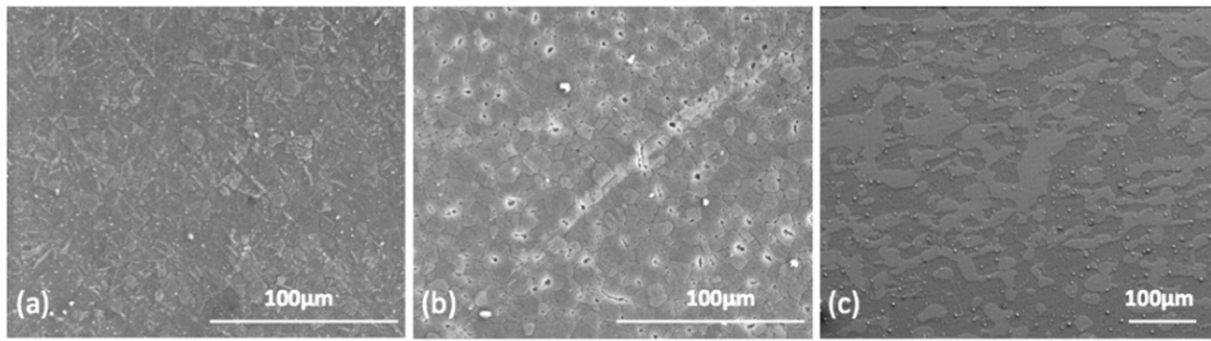


Fig. 1. SEM images showing the typical microstructure of (a) ZN20, (b) NZ20, and (c) Mg-10Li alloy.

higher than those in other two extract groups, while no significant difference was found among all the alloy extract groups. The density of live endothelial cells was almost the same among all alloy extract groups. The live cell densities of osteoblast and endothelial cells cultured in the alloy extract groups were slightly lower than that in the control group (cell culture media with 25 vol% PBS). Among the Mg alloys, the densities of dead osteoblasts in NZ20 and Mg-10Li groups were higher than those in ZN20 and control groups. The densities of dead endothelial cells in NZ20, Mg-10Li and control groups were similar, but were higher than that in ZN20 group. However, no significant differences existed among four groups for both osteoblasts and endothelial cells. Fig. 3(c) reveals the ratio of dead to live cells in different groups. For osteoblasts, the ratios in NZ20 and Mg-10Li groups were higher than those in ZN20 and control groups, but no significant difference could be seen. For endothelial cells, the ratios in all the alloy extract groups and control group were similar ($p > 0.05$). It worth mentioning that the ratios of dead to live cells for different alloy extract groups were lower than 6.5% for osteoblasts and 2% for endothelial cells.

These results suggested that all three Mg alloy extracts showed acceptable cytocompatibility to osteoblasts and endothelial cells at short term (1 day).

Fig. 4(a) and (b) shows the proliferation results of osteoblasts and endothelial cells cultured in different Mg alloy extracts, where the O.D. value was proportional to the viable cell numbers. The cell proliferations of the three Mg alloy extract groups were similar after 1 day, but were lower than that of the control group. The numbers of osteoblasts and endothelial cells were significantly increased in all the Mg alloy groups after 3 and 5 days, and the cell numbers of ZN20 and Mg-10Li groups were higher than that of NZ20 group. After 3 days, both types of cells in NZ20 group exhibited significantly lower proliferation compared with other two groups, while the ZN20 group had the highest proliferation.

Further study on the concentration-dependent cytocompatibility of ZN20 extracts is shown in Fig. 4(c) and (d). For both osteoblasts and endothelial cells, viable cell numbers were not significantly different after 1 day at five concentrations from 12.5 vol% to 66.7 vol%. Even after 3 days, there was no significant decrease in both osteoblast and

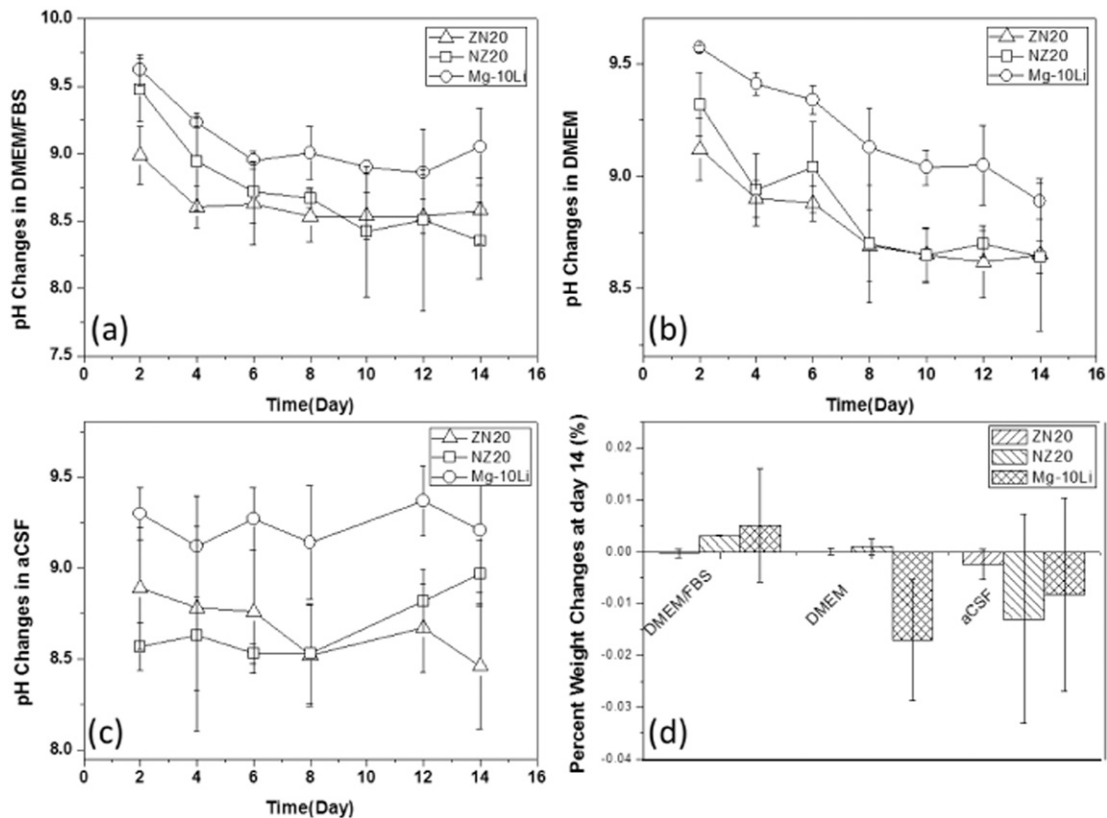


Fig. 2. (a-c) pH changes of the solution containing three Mg alloys: (a) DMEM with FBS, (b) DMEM only, and (c) aCSF, respectively. (d) The change in weight of Mg alloys after immersed in different solutions for 14 days. Data = Mean \pm SD, $n = 3$.

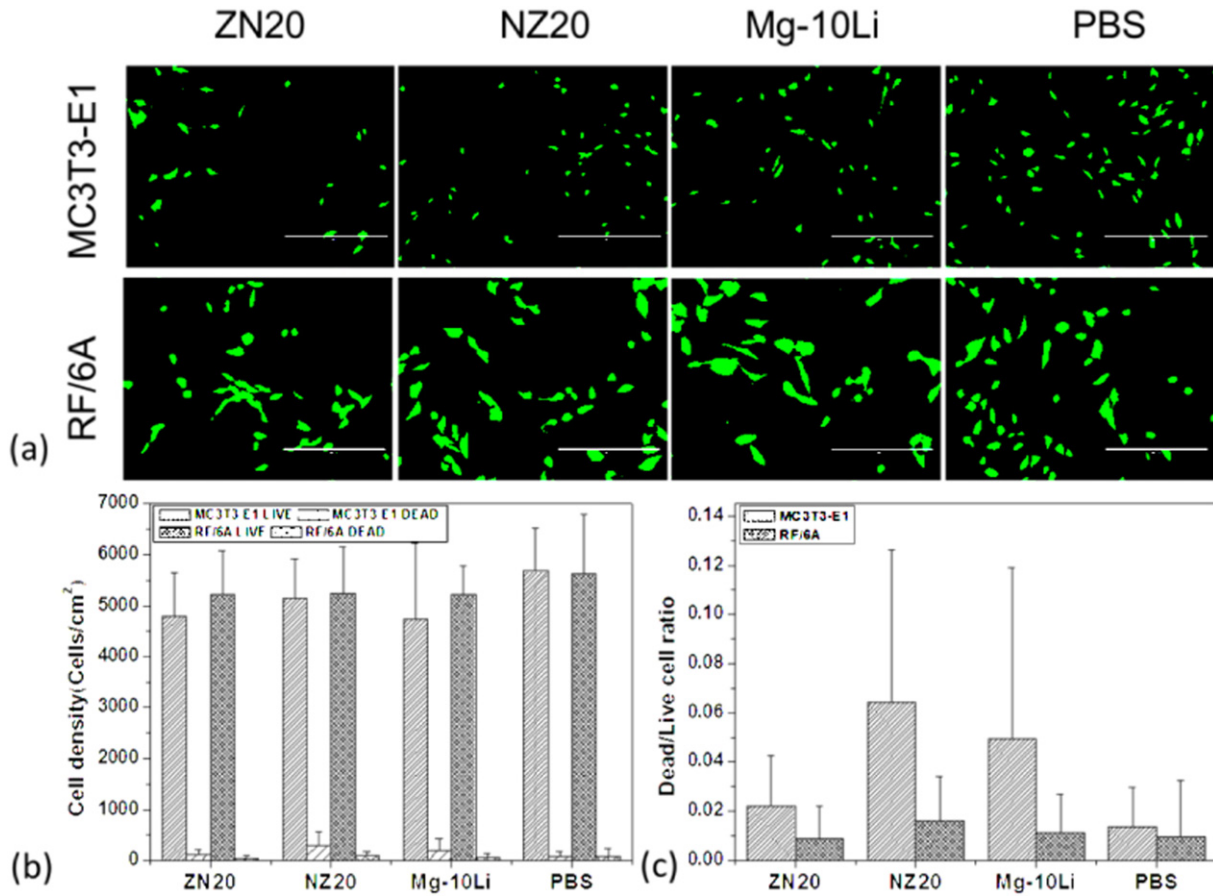


Fig. 3. (a) Fluorescence microscopy images of osteoblasts and endothelial cells cultured in cell culture media supplemented with 25 vol% Mg alloy extracts for 1 day, cells were stained by LIVE/DEAD® assay; (b) live and dead cell density of osteoblasts and endothelial cells in different groups; (c) dead to live cell ratio of osteoblasts and endothelial cells in different groups. No significant difference ($p > 0.05$) was found among the three alloy extracts groups as to the live and dead cells density, and the dead/live cell ratios for the two types of cells. Cell culture media supplemented with 25 vol% PBS was used as the control.

endothelial cell viabilities at concentrations below 50 vol%. However, significant decreases in cell number were observed when the concentration was increased to 50 vol% and above, much lower than the control groups (O.D. values = 0.34 ± 0.03 and 0.18 ± 0.01 for osteoblasts and endothelial cells, respectively). The results suggest that the ZN20 extract at low concentration (<50 vol%) did not have obviously adverse effect on both osteoblast and endothelial proliferations.

3.4. In vitro neurotoxicity

In order to evaluate the neurotoxicity of Mg alloys, DRG neurons were cultured in Mg alloy extracts and their neurite outgrowth lengths were evaluated. A well-known fact is that the longer the neurite outgrowth, the better the viability of the neuron, and the less the neurotoxicity [15].

Fig. 5 (a) shows the typical morphology of DRG neurons cultured with ZN20, NZ20, Mg-10Li extracts and pure cell culture medium (control). DRG neurons in the Mg-10Li and ZN20 extracts had dense and long axons, similar to that of DRG neurons in the control group. In contrast, the DRG neurons cultured with NZ20 extract exhibited much fewer and shorter axons. The results of average maximum neurite length (neuronal extension length) reveal that DRG neurons in Mg-10Li group had the longest neurite among the three experimental groups, followed by ZN20 group, as shown in Fig. 4(b). The maximum neurite lengths in these two groups were also close to that of the control group. However, the maximum neurite length in NZ20 group was significantly less than the control group, indicating potential toxic effect of NZ20 on DRG neuron.

Since the effects of pH and ion concentration on neurons and their related cells have been reported [13,33], pH values and concentrations of Mg^{2+} , Li^+ and Ca^{2+} ions in the Mg alloy extracts were measured (Fig. 5c). NZ20 extract had the highest pH and Mg^{2+} concentration, while ZN20 extract had the lowest pH and Mg^{2+} concentration. The Mg^{2+} concentrations of the three alloy extracts were in accordance with respective pH values, but Ca^{2+} concentration revealed the opposite trend, i.e., $NZ20 < Mg-10Li < ZN20$. This phenomenon was attributed to the Mg degradation-induced pH increase, accelerating the precipitation of Ca^{2+} from cell culture medium into insoluble calcium phosphates. There was considerable amount of Li^+ ions in Mg-10Li extracts, confirming the aforementioned fast degradation of this alloy.

4. Discussion

Ideal materials for NGC application need adequate mechanical strength to support the conduit structure for nerve growth [4,5]. Most of the organic materials currently used for NGC do not have enough mechanical strengths (with tensile strengths usually <1 MPa) to well protect the nerve tissue [17]. The mechanical strengths of Mg alloys are much higher (>50 MPa) than those of the organic counterparts [17–19] and the tensile strengths of the NZ20 and ZN20 alloys used in the present study reach 230 MPa and 200 MPa, respectively. To use Mg alloys as a supporting structure of NGC, the selected alloy should also have good plasticity to fabricate NGC. The NZ20 alloy and ZN20 alloy were used due to their high plasticity: the elongation to fracture was measured to be 20% for extruded ZN20 alloy and 33.4% for extruded NZ20 alloy, respectively. Furthermore, the mechanical properties of Mg-

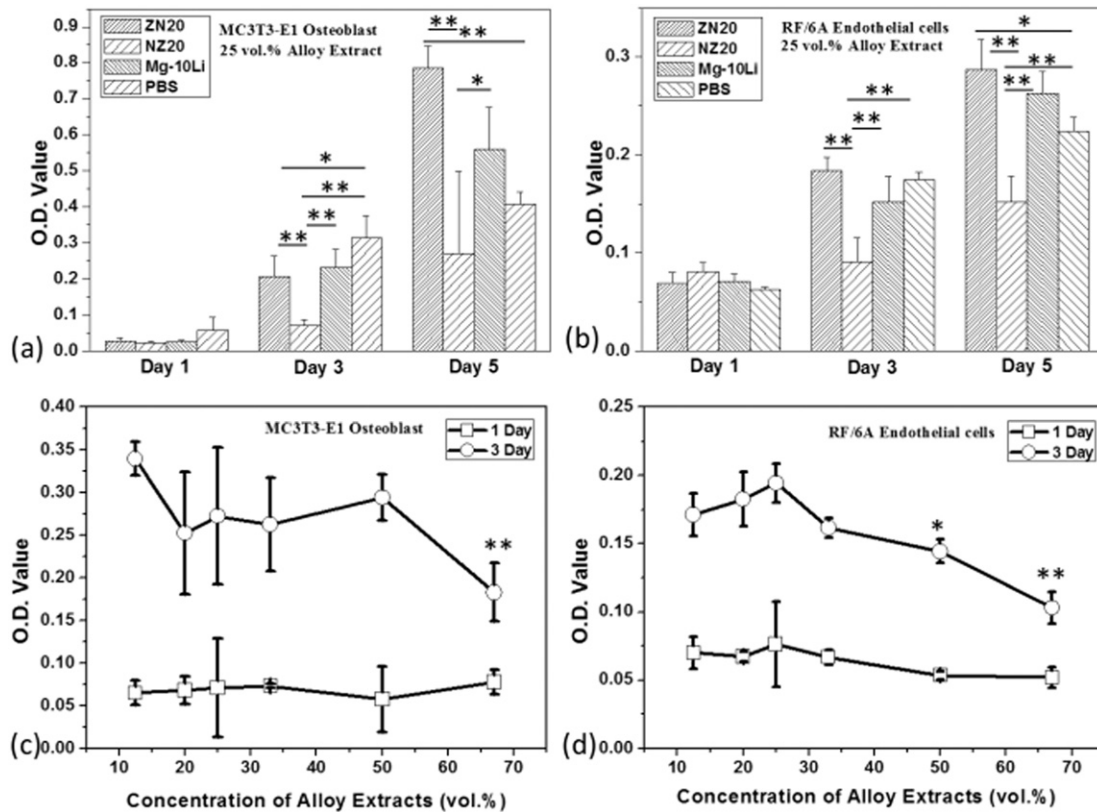


Fig. 4. Results of CCK-8 proliferation assay conducted on osteoblasts and endothelial cells. (a, b) O.D. values of wells with (a) osteoblasts and (b) endothelial cells cultured in different alloy extract solutions for 1, 3, and 5 days, respectively. (c, d) The variation in O.D. values of (c) osteoblasts and (d) endothelial cells cultured in different concentrations of the ZN20 extracts for 1 and 3 days. Data = mean \pm SD, $n = 4$, * $p < 0.05$, ** $p < 0.01$ compared with control group (cell culture media with 12.5 vol% PBS).

based NGC can be optimized by adjusting the structure and configuration of conduit to meet the requirements of nerve repair application [4]. The Mg-10Li alloy was adopted due to the bio-function of Li^+ to nervous system [34–36]. Osteoblasts were used to evaluate the potential toxicity of Mg^{2+} to hard tissue. Choroid-retina endothelial cells are main cells of retina that contact with optic nerve, which may be affected by the released Mg^{2+} when using Mg-based device for optic nerve repair.

4.1. Cyto-compatibility and neuro-toxicity of the alloy extracts

In this work, degradation property, cyto-compatibility and neurotoxicity of several Mg alloys were studied *in vitro* to provide necessary information for their potential applications for neural implants and repair. The extracts of Mg alloys were used to simulate the micro-environment after the implantation of the Mg alloys. In short term (1 day), the results from live/dead and CCK8 assays revealed minimal toxicity of Mg alloys to osteoblasts and endothelial cells. In relatively longer periods of time (3 days), however, the NZ20 alloy extract showed obvious adverse effect on the proliferation of the above two cells compared with the PBS control, which was probably due to the excessively high concentration of Mg^{2+} and Nd^{3+} ions in the extracts [37–39]. Osteoblasts in ZN20 and Mg-10Li extracts groups grew significantly better than that in NZ20 extract group but still worse than PBS control. Endothelial cells in the ZN20 extract showed the highest proliferation that was even higher than that in PBS control, followed by Mg-10Li group, which is comparable to the PBS control. It has been well accepted that cyto-toxic effect of biodegraded products are concentration dependent. The compatibility of different ZN20 extract/medium mixes indicated that the concentration of released ions from ZN20 strongly affected the cell proliferation (Fig. 4c and d), and high concentration of alloy extract (>50 vol%) had inhibitory effect on cell proliferation. It is interesting that, however, the released ions from the degradation of ZN20 alloy appeared to have

positive effect on the proliferation of endothelial cells at a proper concentration (25 vol% in Fig. 4d). In general, only NZ20 extract showed apparent adverse effects on the proliferation of osteoblast and endothelial cells.

In terms of neural toxicity, Mg-10Li extract demonstrated the least neurotoxicity and followed by ZN20 extract, both two extracts revealing similar neural compatibility with control group. However, the NZ20 extract again showed considerable neurotoxicity. The toxic effect of NZ20 alloy extract on DRG was probably due to the excessively high pH [33, 40] and Mg^{2+} ion concentration [13,14,37] caused by the degradation of alloy (Fig. 5c). The Mg-10Li extract showed the best compatibility with DRG neurons though having pH similar to that of ZN20 extract. This is probably owing to the proper Mg^{2+} ion concentration or the effect of Li^+ ions on maintaining neuron activity.

Considering the good cyto-compatibility and negligible neurotoxicity of Mg-10Li alloy and the potential beneficial effect of Li^+ on neural tissue [34–36], Mg-10Li alloy might be a promising biodegradable magnesium alloy for nerve repair. If high plasticity is necessary, ZN20 alloy could an alternate for the fabrication of nerve repair devices. Among the three Mg alloys presently studied, NZ20 alloy seems not appropriate for nerve repair and regeneration applications.

4.2. Effects of alloy composition and degradation rate on cyto- and neural compatibility

It is not uncommon that different Mg alloys exhibited varied cyto-compatibility and neurotoxicity, but the reason behind may be complex. The above results revealed that different Mg alloys had altered degradation rates and varied compositions of the degradation products (outer layers, released ions, etc.), which would simultaneously define a dynamic ionic environment surrounding the Mg alloys after implantation. Previous studies have shown that Mg^{2+} could decrease the neuron

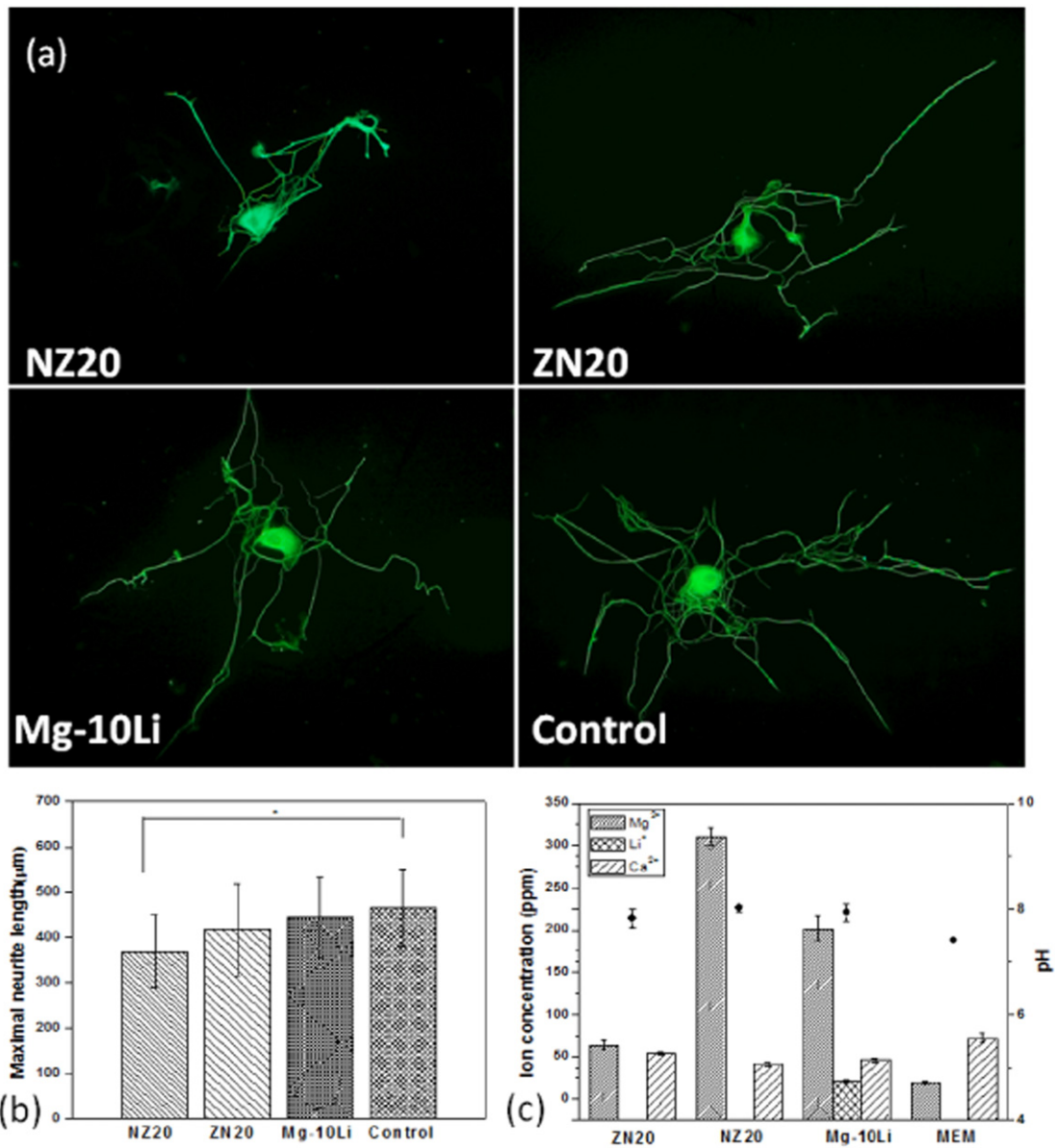


Fig. 5. (a) Typical morphology of DRG neurons cultured with ZN20, NZ20, Mg-10Li extracts and regular cell culture medium (control); (b) average maximum lengths (neuronal extension length) of DRG neurons, Data = average ± SD, n = 10, *p < 0.05; (c) pH values and concentration of Mg²⁺, Li⁺ and Ca²⁺ ions in the Mg alloy extracts.

apoptosis after injury [41] and properly increasing Mg²⁺ concentration in the extracellular fluid could also benefit the viability, proliferation, and growth of neurite of neuronal stem cells [13,14]. Results from present study supported these findings by showing acceptable neuron compatibility in ZN20 and Mg-10Li extracts.

Beside Mg²⁺ ions, Mg alloys are also able to release other alloying elements during degradation, which can also be selected purposely to facilitate nerve repair or regeneration. For example, Li⁺ ions have been proved having protective effect on neurons and ability to enhance remyelination of peripheral nerves [34,35]. Here, Mg-10Li alloy was selected due to the beneficial effect of Li⁺ on the nervous system [35,36]. Considerable amount of Li⁺ ions was indeed released from the Mg-10Li alloy (Fig. 5c) and its concentration (~20 ppm) was expected to be within the range leading to positive effect on nerve regeneration [36]. The neural toxicity test in the present study also supported this expectation by showing that DRG neurons cultured with Mg-10Li extract had the longest neurite lengths compared to other two Mg alloys. In addition, the released amount of Li⁺ ions is adjustable and should be optimized for nerve regeneration in future study.

The degradation profile of the NGC should accommodate the rate of nerve regeneration. Ideally, the conduit should be fully resorbed by the body at the completion time of nerve repair. It is proposed that the NGC would ideally be significantly degrading after the axonal phase (~3 weeks for a 10 mm nerve gap) [42]. In the present study, the degradation of Mg alloys was evaluated by monitoring the pH changes in the soaking solution and weight loss of the samples at the end of immersion test. Considerable degradation was demonstrated by significant pH elevation. However, the results revealed little weight loss, which could be due to the degradation products left on the degradation sites, which is a common phenomenon for Mg alloy during immersion tests and has been reported in previous studies [21,22,30]. The degradation products of Mg alloy could be absorbed *in vivo* through the endocytosis effect of macrophage and the reported degradation rates of biodegradable Mg alloys vary from ~0.1 to ~23 mm/year [18,19]. Theoretically, Mg-based NGC with a wall thickness of 0.5 mm (which is reportedly a suitable thickness for NGC [43]) is expected to degrade completely within a time range from 1 week to 5 year depending on the alloy composition and microstructure. Therefore, the degradation rate of Mg alloy can

probably meet the requirement of nerve repair by adjusting the composition and microstructure. However, it should be noticed that the *in vitro* degradation test just shows a tendency of the Mg degradation rather than the exact degradation behavior *in vivo* [21,44]. It is reported that the degradation rate *in vivo* is significantly greater than the degradation rate *in vitro* [8,45]. Investigation on the *in vivo* degradation rate of Mg alloys by proper animal models is necessary in the further study.

It is worth mentioning that the degradation rate of Mg alloy is directly associated with the surrounding ionic environment [46,47] including pH value [25,47] discussed above, which subsequently affects the neural tissue. The present results clearly show that Mg^{2+} released from NZ20 degradation reached a concentration of 310 ppm (~12.9 mM) and exhibited toxic effect to DGR neurons. This result agreed with a published study, in which the numbers of neural stem cells increased when Mg^{2+} was at 2.5–10 mM, while at 10–20 mM cell numbers decreased, and the concentrations of 40 mM or more resulted in significant neural toxicity [14]. Thus, the Mg^{2+} ion release rate should be maintained at a proper level (<12 mM in this study) by adjusting the Mg alloy composition and its degradation rate. Along this line, this work demonstrated the potential and feasibility of ZN20 and Mg-10Li alloys for nerve repair applications due to their proper degradation behavior and negligible cyto- and neuro-toxicities. However, more *in vitro* and *in vivo* evaluations should be taken to justify the feasibility of Mg alloys for nerve repair. For this purpose the composition and degradation rate of Mg alloy should be optimized in the future. The material development should be based on the nerve regeneration rate and favorable ionic environment for nerve repair. Immersion tests are commonly taken to evaluate the degradation rate of the magnesium alloys in simulated body fluids (Fig. 2). Proper simulated body fluids are critical for well studying the materials properties under the *in vivo* conditions [21,48]. Identification of the simulated body fluids suitable for *in vitro* study of Mg alloys for nerve repair should also be one of the future works.

5. Conclusions

Three Mg alloys, ZN20, NZ20 and Mg-10Li, exhibited significantly varied degradation behaviors in different simulated physiological fluids and altered ionic environments surrounding the alloys. All three Mg alloy extracts at 25 vol% did not induce the significant death of osteoblasts and endothelial cells after 1 day of culture. Only the NZ20 extracts had adverse effect on the proliferation of both types of cells up to 3 days of culture. ZN20 and Mg-10Li extracts showed negligible neurotoxicity on DRG neurons, but NZ20 extract revealed significant neurotoxicity. The ZN20 and Mg-10Li alloys appeared to be promising materials for nerve repair applications, and further *in vitro* and *in vivo* evaluations on these Mg alloys should be performed.

Acknowledgements

The authors would like to thank the National Basic Research Program of China (973 Program, 2014CB748600), the Priority Academic Program Development of Jiangsu High Education Institutions (PAPD), Jiangsu Innovation and Entrepreneurship Program, National Natural Science Foundation of China (51672184, 81622032, 81501858 and 51472279), Jiangsu Provincial Special Program of Medical Science (BL2012004), and the Jiangsu Six Peak of Talents Program (2013-WSW-056) for supporting this work.

References

- [1] A. Bozkurt, F. Lassner, D. O'Dey, R. Deumens, A. Böcker, T. Schwendt, et al., The role of microstructured and interconnected pore channels in a collagen-based nerve guide on axonal regeneration in peripheral nerves, *Biomaterials* 33 (2012) 1363–1375.
- [2] H.-S. Ahn, J.-Y. Hwang, M.S. Kim, J.-Y. Lee, J.-W. Kim, H.-S. Kim, et al., Carbon-nanotube-interfaced glass fiber scaffold for regeneration of transected sciatic nerve, *Acta Biomater.* 13 (2015) 324–334.
- [3] G. Ciardelli, V. Chiono, Materials for peripheral nerve regeneration, *Macromol. Biosci.* 6 (2006) 13–26.
- [4] X. Gu, F. Ding, Y. Yang, J. Liu, Construction of tissue engineered nerve grafts and their application in peripheral nerve regeneration, *Prog. Neurobiol.* 93 (2011) 204–230.
- [5] Y.C. Huang, Y.Y. Huang, Biomaterials and strategies for nerve regeneration, *Artif. Organs* 30 (2006) 514–522.
- [6] F. Witte, V. Kaese, H. Haferkamp, E. Switzer, A. Meyer-Lindenberg, C. Wirth, et al., *In vivo* corrosion of four magnesium alloys and the associated bone response, *Biomaterials* 26 (2005) 3557–3563.
- [7] F. Witte, The history of biodegradable magnesium implants: a review, *Acta Biomater.* 6 (2010) 1680–1692.
- [8] X. Lin, L. Tan, Q. Wang, G. Zhang, B. Zhang, K. Yang, *In vivo* degradation and tissue compatibility of ZK60 magnesium alloy with micro-arc oxidation coating in a transcortical model, *Mater. Sci. Eng. C* 33 (2013) 3881–3888.
- [9] S. Agarwal, J. Curtin, B. Duffy, S. Jaiswal, Biodegradable magnesium alloys for orthopaedic applications: a review on corrosion, biocompatibility and surface modifications, *Mater. Sci. Eng. C* 68 (2016) 948–963.
- [10] S. Kassira, E. Cottrell James, G. Chambers, Magnesium and cobalt, not nimodipine, protect neurons against anoxic damage in the rat hippocampal slice, *Anesthesiology* 69 (1988) 710–715.
- [11] L.-C. Wang, C.-Y. Huang, H.-K. Wang, M.-H. Wu, K.-J. Tsai, Magnesium sulfate and nimesulide have synergistic effects on rescuing brain damage after transient focal ischemia, *J. Neurotrauma* 29 (2012) 1518–1529.
- [12] E. Kaptaoglu, E. Beskonakli, I. Solaroglu, A. Kilinc, Y. Taskin, Magnesium sulfate treatment in experimental spinal cord injury: emphasis on vascular changes and early clinical results, *Neurosurg. Rev.* 26 (2003) 283–287.
- [13] S. Jia, C. Mou, Y. Ma, R. Han, X. Li, Magnesium regulates neural stem cell proliferation in the mouse hippocampus by altering mitochondrial function, *Cell Biol. Int.* 40 (2016) 465–471.
- [14] J.J. Vennemeyer, T. Hopkins, J. Kuhlmann, W.R. Heineman, S.K. Pixley, Effects of elevated magnesium and substrate on neuronal numbers and neurite outgrowth of neural stem/progenitor cells *in vitro*, *Neurosci. Res.* 84 (2014) 72–78.
- [15] X. Yan, J. Liu, J. Huang, M. Huang, F. He, Z. Ye, et al., Electrical stimulation induces calcium-dependent neurite outgrowth and immediate early genes expressions of dorsal root ganglion neurons, *Neurochem. Res.* 39 (2014) 129–141.
- [16] A.N. Koppes, K.W. Keating, A.L. McGregor, R.A. Koppes, K.R. Kearns, A.M. Ziemba, et al., Robust neurite extension following exogenous electrical stimulation within single walled carbon nanotube-composite hydrogels, *Acta Biomater.* 39 (2016) 34–43.
- [17] S. Wang, L. Cai, Polymers for fabricating nerve conduits, *International Journal of Polymer Science* (2010) (Article ID 138686).
- [18] Y.F. Zheng, X.N. Gu, F. Witte, Biodegradable metals, *Mater. Sci. Eng. R. Rep.* 77 (2014) 1–34.
- [19] N. Li, Y. Zheng, Novel magnesium alloys developed for biomedical application: a review, *J. Mater. Sci. Technol.* 29 (2013) 489–502.
- [20] A. Fazel Anvari-Yazdi, K. Tahermanesh, S.M.M. Hadavi, T. Talaei-Khozani, M. Razmkhah, S.M. Abed, et al., Cytotoxicity assessment of adipose-derived mesenchymal stem cells on synthesized biodegradable Mg-Zn-Ca alloys, *Mater. Sci. Eng. C* 69 (2016) 584–597.
- [21] A. Myrissa, N.A. Agha, Y. Lu, E. Martinelli, J. Eichler, G. Szakács, et al., *In vitro* and *in vivo* comparison of binary Mg alloys and pure Mg, *Mater. Sci. Eng. C* 61 (2016) 865–874.
- [22] B. Ratna Sunil, T.S. Sampath Kumar, U. Chakkingal, V. Nandakumar, M. Doble, V. Devi Prasad, et al., *In vitro* and *in vivo* studies of biodegradable fine grained AZ31 magnesium alloy produced by equal channel angular pressing, *Mater. Sci. Eng. C* 59 (2016) 356–367.
- [23] Q. Zhang, X. Lin, Z. Qi, L. Tan, K. Yang, Z. Hu, et al., Magnesium alloy for repair of lateral Tibial Plateau defect in Minipig model, *J. Mater. Sci. Technol.* 29 (2013) 539–544.
- [24] J.-W. Lee, H.-S. Han, K.-J. Han, J. Park, H. Jeon, M.-R. Ok, et al., Long-term clinical study and multiscale analysis of *in vivo* biodegradation mechanism of Mg alloy, *Proc. Natl. Acad. Sci.* 113 (2016) 716–721.
- [25] J. Han, P. Wan, Y. Ge, X. Fan, L. Tan, J. Li, et al., Tailoring the degradation and biological response of a magnesium-strontium alloy for potential bone substitute application, *Mater. Sci. Eng. C* 58 (2016) 799–811.
- [26] W. Sun, G. Zhang, L. Tan, K. Yang, H. Ai, The fluoride coated AZ31B magnesium alloy improves corrosion resistance and stimulates bone formation in rabbit model, *Mater. Sci. Eng. C* 63 (2016) 506–511.
- [27] M. Haude, H. Ince, A. Abizaid, R. Toelg, P.A. Lemos, C. von Birgelen, et al., Safety and performance of the second-generation drug-eluting absorbable metal scaffold in patients with de-novo coronary artery lesions (BIOSOLVE-II): 6 month results of a prospective, multicentre, non-randomised, first-in-man trial, *Lancet* 387 (2016) 31–39.
- [28] D. Zhao, S. Huang, F. Lu, B. Wang, L. Yang, L. Qin, et al., Vascularized bone grafting fixed by biodegradable magnesium screw for treating osteonecrosis of the femoral head, *Biomaterials* 81 (2016) 84–92.
- [29] J. Vennemeyer, T. Hopkins, M. Hershovitch, K. Little, M. Hagen, D. Minter, et al., Initial observations on using magnesium metal in peripheral nerve repair, *J. Biomater. Appl.* 29 (2015) 1145–1154.
- [30] X. Lin, L. Tan, Q. Zhang, K. Yang, Z. Hu, J. Qiu, et al., The *in vitro* degradation process and biocompatibility of a ZK60 magnesium alloy with a forsterite-containing micro-arc oxidation coating, *Acta Biomater.* 9 (2013) 8631–8642.
- [31] X. Lin, X. Yang, L. Tan, M. Li, X. Wang, Y. Zhang, et al., *In vitro* degradation and biocompatibility of a strontium-containing micro-arc oxidation coating on the biodegradable ZK60 magnesium alloy, *Appl. Surf. Sci.* 288 (2013) 718–726.
- [32] M. Bobby Kannan, R.K. Singh, A mechanistic study of *in vitro* degradation of magnesium alloy using electrochemical techniques, *J. Biomed. Mater. Res. A* 93 (2010) 1050–1055.
- [33] A.C.F. GORREN, A. SCHRAMEL, K. SCHMIDT, B. MAYER, Effects of pH on the structure and function of neuronal nitric oxide synthase, *Biochem. J.* 331 (1998) 801–807.

- [34] D.M. Chuang, R.W. Chen, E. Chalecka-Franaszek, M. Ren, R. Hashimoto, V. Senatorov, et al., Neuroprotective effects of lithium in cultured cells and animal models of diseases, *Bipolar Disord.* 4 (2002) 129–136.
- [35] J. Makoukji, M. Belle, D. Meffre, R. Stassart, J. Grenier, G.G. Shackleford, et al., Lithium enhances remyelination of peripheral nerves, *Proc. Natl. Acad. Sci.* 109 (2012) 3973–3978.
- [36] H. Su, T.-H. Chu, W. Wu, Lithium enhances proliferation and neuronal differentiation of neural progenitor cells in vitro and after transplantation into the adult rat spinal cord, *Exp. Neurol.* 206 (2007) 296–307.
- [37] H.M. Wong, K.W. Yeung, K.O. Lam, V. Tam, P.K. Chu, K.D. Luk, et al., A biodegradable polymer-based coating to control the performance of magnesium alloy orthopaedic implants, *Biomaterials* 31 (2010) 2084–2096.
- [38] F. Feyerabend, F. Witte, M. Kammal, R. Willumeit, Unphysiologically high magnesium concentrations support chondrocyte proliferation and redifferentiation, *Tissue Eng.* 12 (2006) 3545–3556.
- [39] F. Feyerabend, J. Fischer, J. Holtz, F. Witte, R. Willumeit, H. Drücker, et al., Evaluation of short-term effects of rare earth and other elements used in magnesium alloys on primary cells and cell lines, *Acta Biomater.* 6 (2010) 1834–1842.
- [40] C.-J. Pan, Y. Hou, Y.-N. Wang, F. Gao, T. Liu, Y.-H. Hou, et al., Effects of self-assembly of 3-phosphonopropionic acid, 3-aminopropyltrimethoxysilane and dopamine on the corrosion behaviors and biocompatibility of a magnesium alloy, *Mater. Sci. Eng. C* 67 (2016) 132–143.
- [41] H. Zhou, Y. Ma, Y. Zhou, Z. Liu, K. Wang, G. Chen, Effects of magnesium sulfate on neuron apoptosis and expression of caspase-3, bax and bcl-2 after cerebral ischemia-reperfusion injury, *Chin. Med. J.* 116 (2003) 1532–1534.
- [42] A.R. Nectow, K.G. Marra, D.L. Kaplan, Biomaterials for the development of peripheral nerve guidance conduits, *Tissue Eng Part B-Rev* 18 (2012) 40–50.
- [43] L.E. Kokai, Y.-C. Lin, N.M. Oyster, K.G. Marra, Diffusion of soluble factors through degradable polymer nerve guides: controlling manufacturing parameters, *Acta Biomater.* 5 (2009) 2540–2550.
- [44] H. Gao, M. Zhang, J. Zhao, L. Gao, M. Li, In vitro and in vivo degradation and mechanical properties of ZEK100 magnesium alloy coated with alginate, chitosan and mechano-growth factor, *Mater. Sci. Eng. C* 63 (2016) 450–461.
- [45] F. Witte, J. Fischer, J. Nellesen, H. Crostack, V. Kaese, A. Pisch, et al., In vitro and in vivo corrosion measurements of magnesium alloys, *Biomaterials* 27 (2006) 1013–1018.
- [46] H. Dong, Q. Li, C. Tan, N. Bai, P. Cai, Bi-directional controlled release of ibuprofen and Mg^{2+} from magnesium alloys coated by multifunctional composite, *Mater. Sci. Eng. C* 68 (2016) 512–518.
- [47] J. Zhang, Z. Wen, M. Zhao, G. Li, C. Dai, Effect of the addition CNTs on performance of CaP/chitosan/coating deposited on magnesium alloy by electrophoretic deposition, *Mater. Sci. Eng. C* 58 (2016) 992–1000.
- [48] A. Witecka, A. Bogucka, A. Yamamoto, K. Máthys, T. Krajčák, J. Jaroszewicz, et al., In vitro degradation of ZM21 magnesium alloy in simulated body fluids, *Mater. Sci. Eng. C* 65 (2016) 59–69.